First International Symposium on Medical Robotics and Computer Assisted Surgery.
Pittsburgh, Penn., September 22-24, 1994

Robotic Control for Dental Subtraction Radiography

Guy Levy[1], Grigore C. Burdea[1], Stanley M. Dunn[1,2], Robert Goratowski[1]

[1] Rutgers The State University
Department of Electrical and Computer Engineering
P.O. Box 0909 Piscataway, NJ 08855-0909

[2] Div of Oral & Maxillofacial Radiology
New Jersey Dental School
Univ of Med & Dentistry of NJ
Newark, NJ 07104

Abstract

Dental digital subtraction radiography requires accurate repositioning of the patient, X-ray source, and film in order to facilitate correct diagnosis of change in bony structures. Mechanical repositioning systems do not allow radiography of anterior teeth, and are uncomfortable for the patient. A new repositioning system that utilizes an X-ray source mounted on a robot arm, coupled with an electromagnetic, six-degree-of-freedom tracking device was developed. The system runs on a Sun SparcStation, and communication between the host and the robot controller is done via a RS232 serial line. An error analysis was performed in order to determine the influence of sensor and robot errors on system accuracy. Experiments showed small errors over the work envelope of the sensor, and no adverse effect due to the presence of metal work in the patient's mouth. The high bandwidth of the sensor allows real time tracking of small movements of the patient's head. Radiographs were taken first using the Robot System, and then compared with radiographs taken using the traditional mechanical occlusal stent approach. Image analysis was subsequently done using a program for re-alignment and subtraction of subsequent radiographs. Initial results show that the robotic system can achieve digital subtraction results at least as good as or better than those using the traditional stent (i.e, mechanical impression) approach.

1 Introduction

Dental radiographs are the most widely used diagnostic tools in dentistry. This remains true in spite of the inherent limitation that they provide only a two-dimensional projection (i.e., view) of the area of interest. For many disease processes this two-dimensional view is sufficient to characterize the pathology and initiate a treatment plan. For detecting the presence or absence of lesions, one need only look at intensity changes in the film (or image if it has been digitized).

Improved dental health has shifted the emphasis toward early detection of disease requiring more exacting instruments. This is evident in the diagnosis and treatment of periodontal disease [15]. The goal is to be able to detect as early as possible, small changes in the bony structure supporting the tooth. If the loss is not caught in time, the result can be tooth loss and continued oral health problems [1].

Studies have shown that disease can be detected earlier and with greater accuracy by looking at the difference between radiographs taken over time, instead of a single radiograph. This "subtraction" technique can be done optically by aligning films or digitally, by digitizing each film first then subtracting corresponding picture elements to compute a difference image. With the advent of personal computers and low cost imaging systems, most work can now be done digitally.

This presents a unique imaging problem. The two radiographs must enclose the same field of the mouth and must be taken with the same geometry. If they are not, then the radiographs cannot be subtracted meaningfully. The purpose of this subtraction is to eliminate the anatomic features not of interest, the so-called *structured noise* in the image. If the imaging geometry is not the same then the visual appearance of the structured noise is different and thus the difference will not be zero.

The goal must be to produce standardized views of the area of interest. Much work to date has been done on mechanical devices to fix the patient and imaging device (X-ray source) in position. The early studies [1], [2] used subtraction to detect lesions in between teeth and in the supporting structure of the teeth. The more recent papers [3, 5] cite applications of digital subtraction to measure bone loss and density changes in the supporting structure of the teeth. Showing the density changes in color [4] improved the diagnosis agreement among observers. In all cases, however, the application papers point out the difficulty in making the initial measurements, the difficulty in reproducing the original imaging

geometry and why this limits the use of digital subtraction radiography.

Digital subtraction radiography requires a system that provides good repeatability and accuracy for patient positioning. Present digital subtraction radiography positioning systems are mechanical, uncomfortable for the patient, and impractical for certain tooth positions. The goal of our research is to implement an approach to this problem that does not require restricting the patient to a specific position, yet maintains the geometric relationship between patient and X-ray source.

2 The X-ray Robotic System

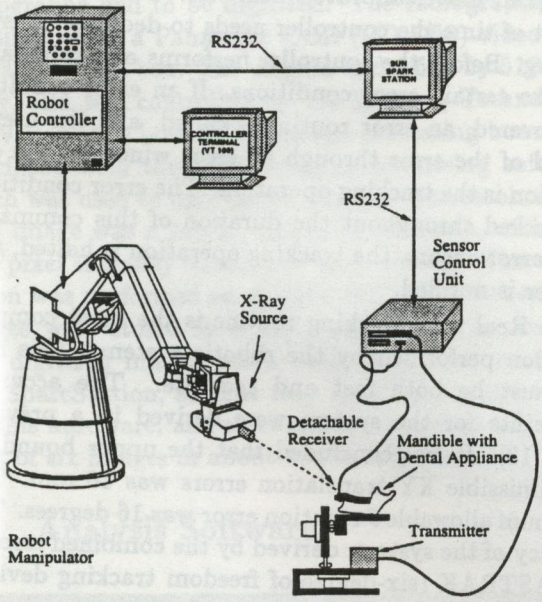

Figure 1: Robotic System

A system was developed to replace present mechanical systems with a sensorized one [12], removing the direct mechanical link between the patient and the X-ray source. The system uses a six-degree of freedom industrial robot coupled with an electromagnetic, six-degree-of-freedom tracking device. The tracking device consists of a Receiver (Sensor), and a Transmitter (see Figure 1). The sensor along with the radiograph film, are mounted on a mouth appliance and allow the robot to track the patient's movements. The robot is equipped with an X-ray device mounted on it's wrist.

2.1 System Hardware

The robot used is a MERLIN [7] six-degree of freedom industrial robot.

The robot's computer [9] is a distributed system that consists of eight independent 6809 microprocessors coordinated by a central 32 bit 8 MHZ 68000 microprocessor. Each of the 6809 microprocessors is dedicated to a single task such as controlling a single robot motor, while the central 68000 microprocessor performs the major computing tasks and coordinates the activity of the 6809 systems. Therefore the central 68000 performs the main motion control calculations, coordinating the movement of joints and determining where each joint should be at every point in time. Every 128 milliseconds, the 68000 system informs each axis control circuit where the robot motor it is controlling should be.

The robot is programmed using the AR-BASIC [8] programming system. AR-BASIC is hosted under MAGIX [7], a UNIX-like operating system. AR-BASIC is a version of the popular language BASIC that contains special robotic extensions.

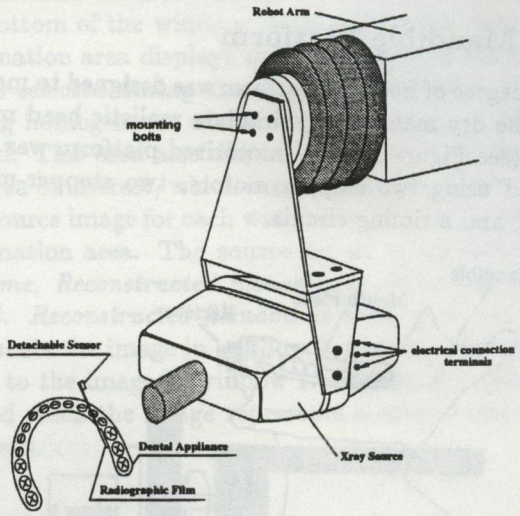

Figure 2: Mounting of X-ray Device

The robot was retrofitted with the GX-1000 intra oral X-ray system made by General Electric [10]. The X-ray device consists of a master controller, and a tube head. The 46lb tube head is mounted on the robot's wrist. The duration and intensity of the X-rays emitted from the tube head are controlled by the master controller. An X-ray can be taken by pressing the hand switch attached to the master controller. The mounting of the X-ray tube, along with the model of the mouth appliance can be seen in Figure 2.

This robot is coupled with Polhemus's FASTRAK sensor, which is an electromagnetic, six-degree-of-freedom tracking device [11].

The robot controller is equipped with analog and digital I/O ports. These ports are used by the system to control/enable various external devices. The Polhemus FASTRAK sensor, for example, is powered through one of the analog output modules. When the associated output module is enabled, power is supplied to the FASTRAK device. The hand switch, used by the X-ray operator, is enabled from one of the digital I/O ports. Therefore all X-ray exposures are initiated by a human operator, but the software enables the hand switch only

when the robot is in the *proper* position. Therefore the robot system does not actually take X-rays, but it regulates the *circumstances* under which, an X-ray may be taken.

The robotic system has also been setup to recognize a digital input signal from an external safety device. The safety device considered during the design of the robotic system was a safety mat that can be triggered by the presence of weight on its surface. One of the digital input ports was setup to record the presence of an input voltage. If this voltage is present, an error routine will be triggered in the robot systems software. This error will halt operation and pass on error information to the user.

2.2 Mandible Platform

A two degree of freedom platform was designed to manipulate the dry mandible to simulate realistic head movements (see Figure 3). The motorized platform was constructed using two stepper-motors, two stepper-motor drivers, and a timing circuit.

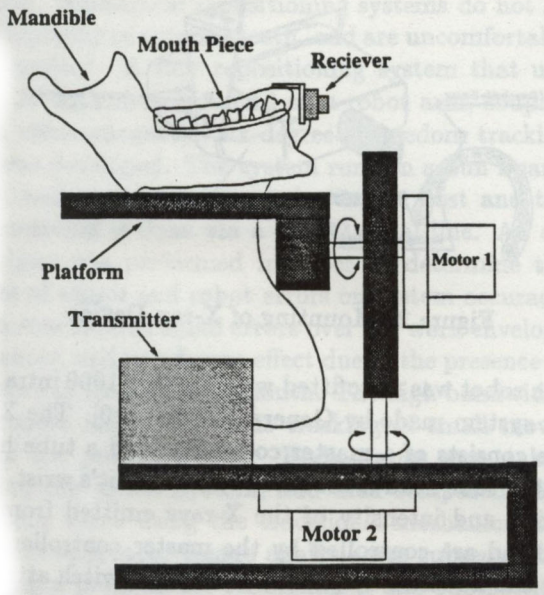

Figure 3: Mandible platform used to simulate head movements

2.3 Graphical User Interface

The main application runs on a UNIX based Sun SparcStation. The graphical user interface was designed under the X Window System [6] Version II, Release 5. The graphical user interface gives the application user total control of the system (see figure 4).

The system is equipped with information feedback, and also error feedback. Feedback windows are responsible for obtaining user input and for passing information on to the user. Error windows are responsible for reporting any error conditions to the user.

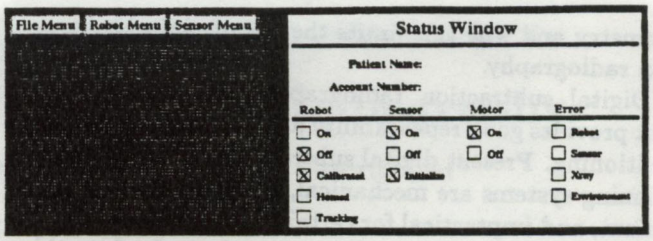

Figure 4: Application Main Screen

Error windows are displayed whenever the software is notified by the robot controller that there is an error somewhere in the system. The majority of errors will come after an attempt to perform some robot command (i.e., move;calibrate;track. etc). This reduces the amount of time the controller needs to dedicate to error checking. Before the controller performs any command, it checks certain error conditions. If an error condition is discovered, an error routine is called, and the user is notified of the error through an error window. The one exception is the tracking operation. The error conditions are checked throughout the duration of this command. If any error occurs, the tracking operation is halted, and the user is notified.

The Real time tracking routine is the most complex operation performed by the robotic system. This routine must be both fast and accurate. The accuracy constraints for the system were derived in a previous study [13]. It was concluded that the upper bound for the admissible XY translation errors was 16 mm. The maximum allowable θ rotation error was 16 degrees. The accuracy of the system, derived by the combined error of the FASTRAK (six-degree-of freedom tracking device), and the robot's positioning error, fell within the requirements set by the previous study.

Many steps were taken to improve the initial response time of the tracking process. Measures were taken to reduce the communication time, and a point server was created. In order to reduce the communication time, a relative reference frame was created, and a compression algorithm was implemented.

The new reference framed was created in the expected neighborhood of the mouth piece and sensor. Once the new reference frame is defined, the robot will perform all move operations relative to the new reference frame. Therefore the reference frame determines the numerical range of the position and orientation values, and thus the length of the communication packet.

In order to assure that the current point information was always available, a point server was created. The server is implemented as a separate process, and runs in parallel with the main application. The server is responsible for performing all necessary point transformations on the current position of the sensor. The robotic system queries the point server whenever it needs the current point information.

Throughout the tracking operation, a status window displays the current status of the robot. The status displayed will be either **TRACKING**, or **LOCKED**. A button will be provided inside the status window, with which the user may halt the tracking operation.

This design assumes that (for safety reasons) the X-ray will be activated manually, by means of an external button, activated by the Dentist or technician (not the software). The external X-ray button, will however be *enabled* by the software, whenever the robot has **LOCKED** onto the sensor.

2.4 Imaging Equipment

In order to perform the digital subtraction analysis, the radiographs had to be digitized. The radiographs were digitized using a Panasonic CCD (CD-D50) video camera, and a light box. The camera had a 512 by 512 CCD array, and was controlled by the Imaging Technologies PC Vision Plus board. The image processing board was interfaced with the TIPS imaging processing software, which was used to digitize the images. The resolution of each image was a 240 by 256 array of pixels, with an 8 bits/pixel intensity value (256 gray levels). The digitization was performed on an IBM PC/AT. The resulting images were stored in a raw format with no headers. The digitized images where later transfered over to a Sun SparcStation, so that they could be analyzed. Using this hardware, and software, it is possible to digitize a set of six images in about twelve minutes.

2.5 Analysis Software

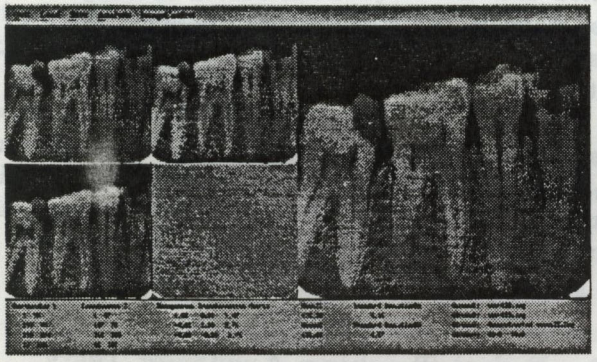

Figure 5: Digital Subtraction Software

The analysis software was created under X-Windows, using the MOTIF widget set (see Figure 5), on a Sun SparcStation. The Sun SparcStation has a grayscale monitor capable of displaying the high resolution grayscale images.

Image registration is used in order to remove the effects resulting from the differences in imaging geometry. The resulting images will appear to have been formed with the object, the X-ray source, and the recording planes, all in equivalent positions. If the image is a two dimensional object, image registration can always be performed, as there is a one-to-one mapping of object points to image points. This relationship does not hold for three dimensional objects. Image registration may however be done on the two dimensional projections of three dimensional objects. In order for a meaningful subtraction, certain restrictions must be followed. These restrictions were derived in a study based on algorithms used to *force* spatial correspondence [16]. The results of the study showed that successful image registration can be performed on images with less than a 16mm translation error and angulation errors of up to 16 degrees.

The main application window can display up to five images, four 240 by 256 images, and one 480 by 512 image. A menu bar is located at the top of the window. At the bottom of the window, is an information area. This information area displays the coordinates of the feature points selected during the registration routine. The resulting homogeneous transformation matrix is also displayed. This area also displays the statistical results of the area of interest, which is set in the statistics window. The source image for each window is also displayed in the information area. The source for an image will be the *filename*, *Reconstructed filename*, or *Window# - Window#*. *Reconstructed filename* is used when the image represents the image in window 2, standardized with respect to the image in window 1. *Window# - Window#* is used when the image represents a subtraction of two windows.

3 Experimental Results

3.1 Polhemus Accuracy & Repeatability

The first experiment was to determine the Polhemus Fastrack accuracy and repeatability over its work envelope.

The sensor readings were compared to the correct values measured manually, directly on the calibration table [16]. The calibration table has a large millimeter spaced grid, which allows us to measure the sensor location within millimeters. The test data for the Fastrack is shown in Figure 6. The solid line represents the accuracy error data while the dashed line is the possible mouthpiece position. 1,000 readings were made and averaged for each position in order to suppress sensor noise.

Subsequently the same series of tests were performed, at different locations on the calibration table. These tests were made to determine if there is significant degradation of sensor measurements as the distance between sensor and source increases. In the dental applications the source is fixed on the back of the X-ray chair, or in some other convenient location. The optimum sensor range was determined to be well over the distance that the sensor will have from the source. Within this range, the sensor readings differ by at most 1 mm Euclidean translation (radial distance) and 1 degree total rotations, when compared to the correct values.

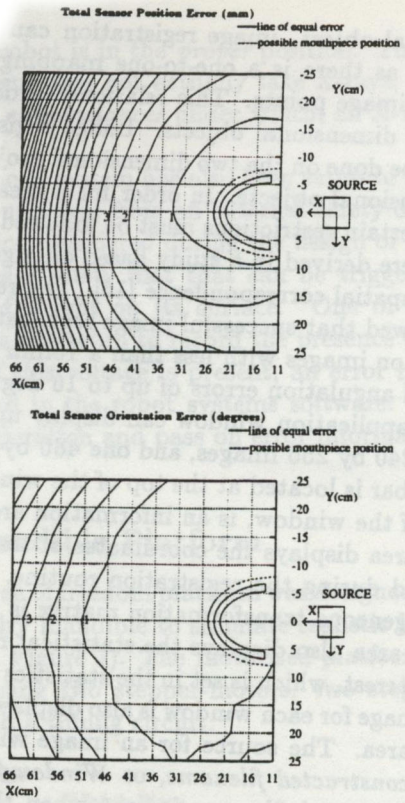

Figure 6: Sensor Readings Over Work Envelope

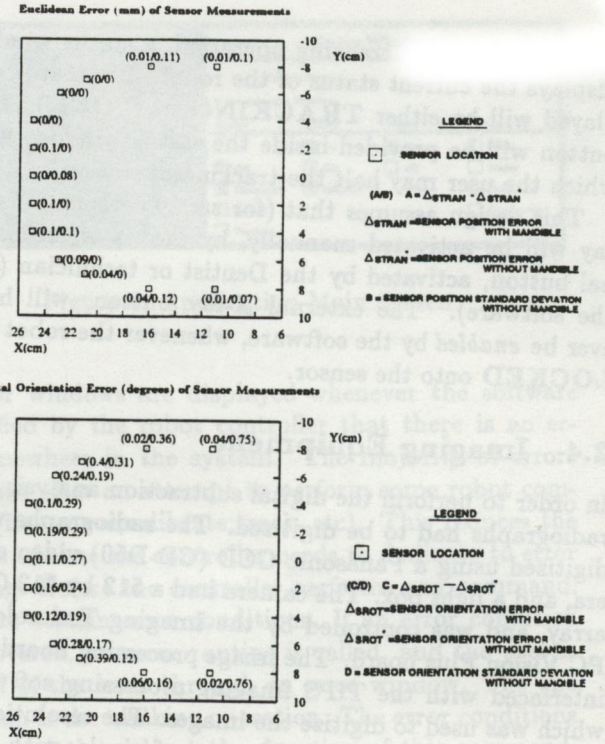

Figure 7: Sensor Readings With The Dry Mandible With Orthodontic Metal

The larger errors are due to a relatively imprecise calibration table. Thus the "correct" values had a built-in reading error of about 0.5 to 1.0 mm. According to its manufacturer, sensor measurements are not affected by X-rays.

The experimental results on the Isotrack [12] and the newer Fastrack sensor errors satisfy the necessary constraints. Under these conditions, translation errors (Δ_{stran}) are 1 mm or less for a sensor to source distance of 200 mm. Since this is within the optimal range for the application, these results are very encouraging. Figure 6 shows the Fastrack position and orientation errors over the sensor work envelope.

3.2 Effect of Metal on Sensor Readings

A second set of measurements were performed to determine if there is a significant degradation of sensor readings due to the presence of metal (i.e., restorations and orthodontic appliances) in the patient's mouth. An initial set of readings were done for all six DOF with a dry mandible that had no metal and the Isotrack. These readings showed that there is no difference in data when the skull was interposed between the source and the sensor block, or when it was not (the difference was on the order of the sensor noise). Subsequently, the same mandible was fitted with orthodontic wire and 10 amalgam restorations and the same measurement procedure was applied. Then the same mandible was interposed between the Fastrack and its source.

The measured translation error with the mandible present was Δ_{stran}, while the same error without the mandible was $\Delta_{stran}*$. The two sets of data were subtracted and the difference compared with the sensor noise standard deviation at that location. The results illustrated in Figure 7 show that there is no significant change in sensor accuracy due to the metal in the mandible. The same test was repeated for sensor rotation errors as shown in Figure 7. The maximum $\Delta_{stran} - \Delta_{stran}*$ was 0.1 mm while the maximum noise standard deviation was 0.12 mm. This indicates that there is no adverse influence on sensor accuracy due to the presence of metal in the patient's mouth.

3.3 Robot Tracking Accuracy Tests

The dynamic tests used to determine the accuracy of moving target tracking yielded promising results. In normal operation the moving target is the patient's head. The range and velocity of head motions are known. and therefore our tests provide realistic simulations of the movement of the head by changing sensor data. In addition to the sensor feedback, the robot is equipped with a directed light source for visual feedback. This directional light source was used to help fine-tune the robot calibration.

The accuracy tests were performed by mounting the

sensor on a millimeter grid, supported by a stand with three degrees of freedom. The desired position and orientation of the X-ray source with respect to the sensor receiver is set in the tracking applications data resource file (SensorPosition.dat). This allows for the flexibility of changing the target point at which the X-ray source aims. The desired point is marked on the grid. A laser pointer mounted inside a plastic tube coaxial with the X-ray beam (X-ray's x-axis) is used to visualize the X-ray source's target.

The tracking procedure involved aiming the laser pointer at the sensor grid, and then rotating and translating the sensor mounted on the grid. In the absence of errors, the laser pointer should not change position on the grid. Throughout the experimentation, a repeatability error of about 1 mm was observed. The tracking error remained at one millimeter also.

3.4 X-ray Subtraction Tests

Three sets of experiments were performed in which actual X-rays were taken. A total of 57 radiographs were produced using the GE X-ray machine and the robotic system.

Value	Mean	Stn Dev	X (p)	Y (p)	Y (θ)	X (θ)
Avg	127.25	3.85	2.85	2.59	0.01	0.01
Min	122.25	3.01	0.10	0.00	-0.00	-0.00
Max	132.22	4.67	6.56	10.51	0.05	0.04

Table 1: Total Robotic System Results

Value	Mean	Stn Dev
Avg	127.24	5.91
Min	122.07	3.51
Max	132.41	8.68

Table 2: Total Straight Robotic System Results

During the first experiment, four radiographs were taken and these radiographs were used for calibration. The current, voltage, and exposure times were set during this stage of the experiment. The final settings resulted in a current of 10 mA, a voltage 70 kVp, and a fixed exposure time of 12 60th's of a second. These settings determine the quality of the resulting radiograph, and if set incorrectly can result in a radiograph in which features can not be properly discerned. The kVp settings for example can be used to control the contrast in the resulting radiograph. High kilovoltage peak (kVp) exposures produce a long grey scale with many shades of grey (information), but it may be difficult to perceive a difference between two adjacent regions if the difference is small. Low kVp exposures produce a short grey scale with fewer shades of grey (less information), but may make it easier to detect differences between adjacent regions [14].

Value	Mean	Stn Dev	X (p)	Y (p)	Y (θ)	X (θ)
Avg	127.24	4.27	4.51	3.72	0.02	0.02
Min	114.14	3.12	0.09	0.01	0.00	0.00
Max	140.33	6.34	12.70	10.72	0.07	0.06

Table 3: Total Stent Results

Value	Mean	Stn Dev
Avg	127.25	7.46
Min	114.19	3.95
Max	140.31	13.45

Table 4: Total Straight Stent Results

(a) Vertical Shift +10 (b) Vertical Shift -10

Figure 8: Image #41 (shifted ± 10) subtracted from image #40

Figure 8 displays two subtraction images. The coordinates for the feature positions used in these images have an intentional vertical offset. Image (a) in figure 8 shows the subtraction that results when the Y coordinate of each feature point in radiograph #41 is shifted by +10. This incorrect selection of feature points results in a shift in the standardized image of radiograph #41, which simulates a growth in the bony structure. The white regions in image (a), correspond to the increases in the bony tissue. The results shown in image (b) are similar, however the light region is replaced by a dark region. This dark region results when the Y coordinate of the feature points is offset by -10. This negative offset simulates a loss in the bony structure.

These two examples illustrate the need for proper registration of images. Note also that the greater the difference between the imaging geometries of the two radiographs, the more difficult it becomes to properly register the feature points. In addition, if the imaging geometry is so different, that translation errors of more than 16mm and angulation errors of more than 16 degrees occur, then the image cannot be properly registered. If the X-ray system cannot satisfy these error constraints, it will not be possible to discern the difference between image geometry errors, and valid pathological changes.

The standardization procedure requires four invariant points in order to standardize an image. These points are expected to lie in the same plane. Using these points, a homogeneous transformation matrix is created, that represents a synthesis of the imaging geometry that created the two films. This matrix is used to create the standardized image used in the subtraction process. Therefore the elements of the matrix reveal a quantitative measure of the position and orientation variations from one image to the other.

The second and third experiments were used to compare the subtraction results achieved by radiographs taken with the traditional occlusal stent[1], and those taken with the robotic system. Throughout experiment #2, mouth appliance #1 was used. This mouth piece has a film placement that allows for X-raying of the right posterior teeth of the dry mandible. With this mouth piece, X-rays of the right first and second pre-molars, along with the right first and second molars, were possible. An example of a subtraction using these two methods can be seen in Figure 9.

X-rays taken during experiment #3, were taken with mouth pieces #2 and #3. Mouth piece #2 allowed X-rays of the left and right, central and lateral incisors to be taken. Mouth piece #3 allowed X-rays of the right first, second, and third molar to be taken.

The overall results are tabulated in Table 1 through 4. The average mean is the average intensity value of the resulting pixels in the subtraction image. The standard deviation refers to the standard deviation of the resulting pixel intensities. The translation values correspond to the necessary X, and Y translations, in number of Pixels (p), needed to force the spatial correspondence of features. Similarly, the $Y(\theta)$ and $X(\theta)$ components correspond to the necessary rotation, and shear along the Y axis, and the necessary rotation and shear along the X axis respectively.

In order to provide further proof of the robotic systems accuracy, the statistics resulting from *straight* subtractions are provided. These subtractions are done on the original digitized images. These statistics represent the mean and standard deviation achieved without the use of the re-alignment software.

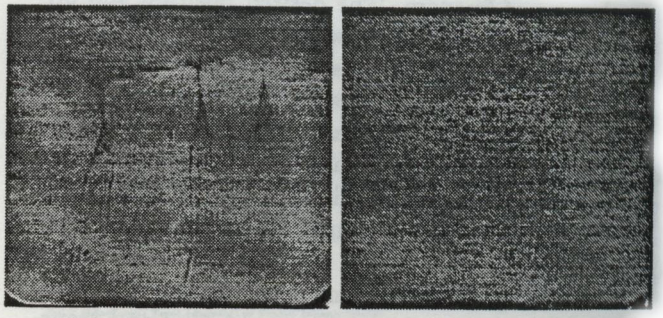

(a) Occlusal Stent (b) Robotic System

Figure 9: Subtraction Images

In practice we notice that there will be some differences between two radiographs taken with the same dry mandible. Some of these errors, can be attributed to digitization noise and digitization placement. Other errors can be contributed to slight changes in the imaging geometry. These errors are due to slight changes in film placement, slight drifts of the robot arm, and precision errors in the robot's tool-tip calibration routine. All of these errors should be removed when the standardization routine is used. Note however, that the standardization routine itself may introduces errors. The results achieved by using the standardization routines are limited by the operators ability to precisely locate the invariant features in each of the digitized radiographs. If the image is not registered properly, the transformation between the two images can not be calculated precisely.

Analyzing the results in Table 1 through 4, we can see that the robotic system achieves results better than those achieved by using the mechanical attachments. In addition, the robotic system yields results that are more consistent than the results achieved by using the occlusal stent. This can be confirmed by looking at the variations in the minimum, maximum, and average values.

One can readily see the result of these errors in the images shown in Figure 9. Slight translations and inconsistencies in the geometric relationship of the X-ray source to the X-ray film can be seen easily in the resulting image. These areas can be falsely interpreted as either bone growth or bone loss. (The interpretation depends on the standard used in the subtraction algorithm.)

The mean value of the intensities in the subtracted image (taking into account image noise) should be close to zero (127 when scaled to a value from 0→255). Both methods had a mean value close to 127. The robotic system however has a minimum and maximum value that is closer to the average mean (a better average standard deviation). The translation and rotation/shear components needed to force the spatial correspondence are also smaller when the robotic system is used.

The "straight" subtraction statistics also reveal the superior performance of the robotic system. Again the

[1] An occlusal stent is a mechanical registration system that is based on reproducing the position of the film with respect to the occlusal, i.e, biting surface of the posterior teeth. A stent is a molded impression of the surface that is reused longitudinally.

average mean values are similar, yet the minimum and maximum mean values are closer to the average mean value in the robotic system case. The robotic sytem also shows an improvement in the standard deviation statistics for the straight subtraction.

As expected, the robot's excellent repeatability, and accuracy led to smaller translation and orientation errors. This reduction guarantees that the standardization and subtraction software will be able to properly re-align and subsequently subtract the two images. Therefore there is a higher degree of certainty that the variations in the two images are attributed to either bone loss or bone growth, and not to inconsistencies in the positioning of the patient with respect to the X-ray source.

4 Conclusion

A robotic system that allows accurate measurement of targeted tooth position without supplemental mechanical alignment was realized. This system avoids direct mechanical contact between the X-ray source and the patient, and therefore can be used to image anterior as well as posterior teeth (mechanical techniques apply to posterior teeth only).

The results achieved using the robotic system look promising. When the re-alignment software is utilized, the robotic system yields results at least as good as or better than those achieved using the traditional occlusal stent approach. Thus the robot's accuracy and repeatability have been proven to aid in the digital subtraction radiography process.

Future work aims at providing a statistical analysis based on more X-ray images taken with stents and with the robotic system.

5 Acknowledgments

Research reported here was supported by Grant PHS 1-R03-DE10230 from the National Institute of Health and by a Grant from the University of Medicine and Dentistry of New Jersey.

References

[1] Ortman L., R. Dunford, K. McHenry, and E. Hausmann, "Subtraction radiography and computer assisted densitometric analyses of standardized radiographs," *J. Periodont. Res.*, vol. 20, pp. 644-651, 1985

[2] Rethman M., U. Ruttiman, R. O'Neal, R. Webber, A. Davis, G. Greenstein, and S. Woodyard, "Diagnosis of bone lesions by subtraction radiography," *J. Periodont. Res.*, vol. 56, pp. 324-329, 1985

[3] Bragger U., "Digital imaging in periodontal radiography" *J. Clin. Periodont.*, vol. 15, pp. 551-557, 1988

[4] Bragger U., L.Pasquali, "Color conversion of alveolar bone density changes in digital subtraction images," *J. Clin. Periodont.*, vol. 16, pp. 209-214, 1989

[5] Bragger U., L.Pasquali, H. Weber, and K. ornman, "Computer-assisted densitometric image analysis for the assessment of alveolar bone density changes in furcations, " *J. Periodont. Res.*, vol. 16, pp. 42-52, 1989

[6] *X Windows System User's Guide*, Version II, Release 5, O'REILLY & ASSOCIATES, INC., June 1985.

[7] *Merlin System Operator's Guide*, Version 3.0, AMERICAN ROBOT CORPORATION, June 1985.

[8] *AR-BASIC Programming Guide*, Version 3.0, AMERICAN ROBOT CORPORATION, June 1985.

[9] *Service Manual for the System II Merlin Intelligent Robot*, Manual No. MSII-SER, AMERICAN ROBOT CORPORATION, February 1985.

[10] *Gx-1000 Intra Oral X-ray System Installation and Maintenance Manual*, Direction No.14544, GENDEX CORPORATION.

[11] *3SPACE FASTRAK User's Manual*, POLHEMUS, A KAISER AEROSPACE & ELECTRONICS COMPANY, OPM3609-002B, November 1992.

[12] Burdea G., S. Dunn, C. Immendorf and M. Mallik, "Real-Time Sensing of Tooth Position for Dental Digital Subtraction Radiography with a Sensorized Dental Mouthpiece and a Robotic System", *IEEE Transactions on Biomedical Engineering*, Vol. 38, No. 4, April 1991;366-372

[13] Dunn S. and P. van der Stelt, "Recognizing Anatomic Structure in Arbitrary Radiographic Projections", *Dento Maxillo Facial Radiology.*

[14] Dunn S. "Digital Standardization of Dental Radiographs" VU University Press, Holland, 1993;0,5:7-9,92-94

[15] Lurie AG, Greenberg RJ, Kornman, KS. Subtraction radiology demonstrates crestal bone loss in experimentally induced marginal periodontitis. Oral Surg Oral Med Oral Pathol 1983; 55:537-41.

[16] Dunn S., G. Burdea, R. Goratowski, "Robotic Control of Intraoral Radiography", in *Computer Integrated Surgery*, MIT Press, (accepted), 1994.